Journal of Catalysis **193,** 171–175 (2000)
doi:10.1006/jcat.2000.2917, available online at http://www.idealibrary.com on IDEAL®

PRIORITY COMMUNICATION

Direct Measurement of Polymer Growth Rate in a Model Ziegler–Natta Polymerization System Using Laser Reflection Interferometry

Seong Han Kim,* Gerard Vurens,† and Gabor A. Somorjai*,[1]

*Department of Chemistry, University of California at Berkeley and Materials Science Division, Lawrence Berkeley National Laboratory, Berkeley, California 94720; and †HDI Instrumentation, 2450 Scott Boulevard, No. 300, Santa Clara, California 95050

Received April 26, 2000; accepted April 27, 2000

The polymer growth rate for polypropylene and polyethylene was measured, for the first time, during polymerization on a model Ziegler–Natta catalyst film with a surface area of ~1 cm^2 by laser reflection interferometry. This technique is based on the difference in the refractive indices of the catalyst and the growing polymer film. A thin film of $TiCl_x/MgCl_2$ deposited on a polycrystalline gold foil was used as a model catalyst. Polyethylene grew about 30 times faster than polypropylene. The changes in periodicity of the interference fringes indicated a slow decrease in the growth rate with increasing polymer film thickness. This may be due to the monomer diffusion that was controlled by the thickness and morphology of the growing polymer film.

Key Words: **Ziegler–Natta; $TiCl_4$; $MgCl_2$; polymerization kinetics; deactivation; laser reflection interferometry.**

I. INTRODUCTION

Kinetic studies of heterogeneous polymerization processes are of fundamental importance to elucidate how polymerization proceeds on the catalyst surface (1, 2). For the high-yield Ziegler–Natta polymerization catalysts used industrially to produce polyolefins, polymerization rates can be obtained by monitoring the monomer pressure decrease (reactant consumption) as a function of polymerization time. However, uncertainties about the surface area and the number of active sites in the microporous catalysts make the quantitative analysis of kinetic data difficult. The situation is further complicated by the existence of multiple active sites (1, 2).

The use of a well-characterized model catalyst could reduce these uncertainties about the surface area and the active site concentration in kinetic analysis (3–5). For polymerization studies of ethylene and propylene, we have prepared model catalysts that were thin films of $TiCl_x/MgCl_2$ deposited from the vapor phase on a gold foil (4–8). The surface areas of these model catalysts were on the order of 1 cm^2. However, the difficulty in accurately measuring the polymerization rate was a main barrier for kinetic studies of polymerization on the well-characterized model catalyst. Since the pressure decrease due to polymerization is negligible compared to the initial pressure of the monomer (typically ≥760 Torr), the monomer consumption rate measurement cannot be made accurately. For example, if 10% of the surface species of a 1-cm^2 catalyst are active sites (~10^{14} sites/cm^2) and each active site polymerizes 10^4 monomers, then the total number of monomer molecules consumed will be 10^{18} molecules. In a reactor of 100 ml, it will cause a pressure drop of ~0.3 Torr, which corresponds to less than 0.04% of the initial pressure (760 Torr).

In this study, we introduce a new nondestructive *in situ* technique—laser reflection interferometry (LRI)—to measure the increasing thickness of the growing polymer film as a function of time. Since the LRI measures the product (polymer) formation, not the reactant (monomer) consumption, the kinetic studies of ethylene and propylene polymerization were possible on a small-surface-area catalyst without interference from the gas-phase monomer molecules. The model catalyst was produced as a thin film form by chemical vapor deposition of Mg and $TiCl_4$ on a polycrystalline gold foil. The ethylene polymerization rate was about 30 times higher than the propylene polymerization rate. Both polymerization rates were on the same order of magnitude as polymerization rates of the industrial catalysts. The changes in periodicity of the interference fringes indicated a slow decrease of the growth rate with increasing polymer film thickness. This may be due to the monomer diffusion that was controlled by the thickness and morphology of the growing polymer film. The work opens opportunities to bridge the polymerization kinetics of the model polymerization catalyst system with its microscopic surface properties.

[1] To whom correspondence should be addressed.

0021-9517/00 $35.00

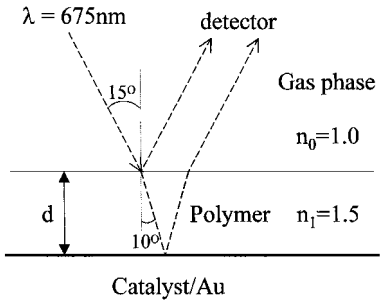

FIG. 1. Schematic representation of the geometry for laser reflection interferometry.

II. EXPERIMENTAL

A. LRI Measurements

The polymer film growth on the model catalyst during polymerization was monitored by the optical interference of a reflected laser beam as schematically shown in Fig. 1. The diode laser ($\lambda = 675$ nm) was incident on the growing polymer film at near normal incidence ($\theta_0 = 15^\circ$). The resulting reflections from the gas–polymer and polymer–catalyst interfaces led to constructive and destructive interference in the reflected laser beam. This reflectance was monitored as a function of polymerization time with the photodetector interfaced with a computer. The near normal incidence was chosen for two reasons: (i) no need to separate the s- and p-polarizations and (ii) applicability to a surface that is not optically flat.

The thickness of the polymer film at time *t*, *d(t)*, can be calculated by simulating the data using the Fresnel equations (9). However, the surface film roughness and density inhomogeneity of the polymer film cause scattering of the laser and complicate the simulation (9). Instead, the polymer film thickness at each peak of the interference oscillation, $d_m(t_m)$, could be easily obtained from the requirement for constructive interference,

$$d_m(t_m) = m\lambda \cdot \cos\theta_1 / 2n_1 \qquad [1]$$

where m is the number of periods of oscillation, $\lambda = 675$ nm, θ_1 is the laser beam propagation angle with respect to the surface normal determined from Snell's law, $n_0 \cdot \sin\theta_0 = n_1 \cdot \sin\theta_1$ ($n_0 = 1.0$ and $\theta_0 = 15^\circ$), and n_1 is the refractive index of the polymer film. Given typical refractive indices of polyethylene and polypropylene of $n_1 = 1.50$–1.55 (10), one full cycle of oscillation between adjacent maxima corresponded to ~222 nm. The polymerization rate was obtained by multiplying the time derivative of $d_m(t_m)$, $\Delta d_m/\Delta t_m$, with the surface area of the model catalyst (A) and the density of the polymer product (d):

$$\text{polymerization rate (g/s)} = \Delta d_m/\Delta t_m \times A \times d. \qquad [2]$$

Typical densities of polyethylene (PE) and polypropylene (PP) grown with the Ziegler–Natta catalysts are 0.96 and 0.91, respectively, at 25°C (11, 12). The actual density of the as-grown polymer film could be slightly different due to porosity and dissolved monomer gases in the polymer film. The thermal expansion of polymer film at the polymerization temperature (70°C) could also cause a small error (less than 5%) in the polymer density approximation (13).

B. Vacuum Chamber

The ultrahigh vacuum chamber, used for fabrication and characterization of the model catalysts, has been described in detail elsewhere (4). Briefly, the apparatus consisted of a preparation chamber, an analysis chamber, and a polymerization reaction cell. The reparation chamber was equipped with an argon ion sputter gun, a magnesium source (Knudsen cell), an electron gun, and leak valves for gas introduction. The analysis chamber housed a PHI 5400 ESCA system for XPS measurements. The reaction cell was equipped with a temperature-controlled diode laser ($\lambda = 675$ nm) and a photodetector for *in situ* LRI measurements of polymer film growth. The model catalyst sample under study was transferred from one section of the apparatus to the others without exposure to air.

C. Catalyst Fabrication and Polymerization

The $TiCl_x/MgCl_2$ model catalyst film was fabricated by co-deposition of $TiCl_4$ and Mg on an Au foil (1 cm^2) at 300 K in the preparation chamber. The details have been published elsewhere (5). The chemical composition of the catalyst film was confirmed with XPS. Then, the $TiCl_x/MgCl_2$ model catalyst film was transferred into the reaction cell (heated to 340 K) and activated by exposure to 5 Torr of $AlEt_3$. Polymerization was carried with 900 Torr of ethylene or propylene.

III. RESULTS AND DISCUSSION

A. Polymer Film Growth

The co-deposition of Mg and $TiCl_4$ produced a thin film that consisted of titanium chloride species ($TiCl_x$) on top of $MgCl_2$ multilayers (5). The reactions of this $TiCl_x/MgCl_2$ film with the $AlEt_3$ co-catalyst were first monitored with LRI. When the $TiCl_x/MgCl_2$ catalyst film was exposed to 5 Torr of $AlEt_3$, the LRI signal intensity decreased slightly due to adsorption of $AlEt_3$ on the film surface. After the excess $AlEt_3$ was pumped out, the LRI signal did not recover to its original value, indicating that the refractive of the catalyst surface was changed as a result of the reduction and alkylation of titanium ions on the catalyst surface by $AlEt_3$ (2). Once treated with $AlEt_3$, the model catalyst film was active for α-olefin polymerization, regardless of the presence of the co-catalyst in the gas phase.

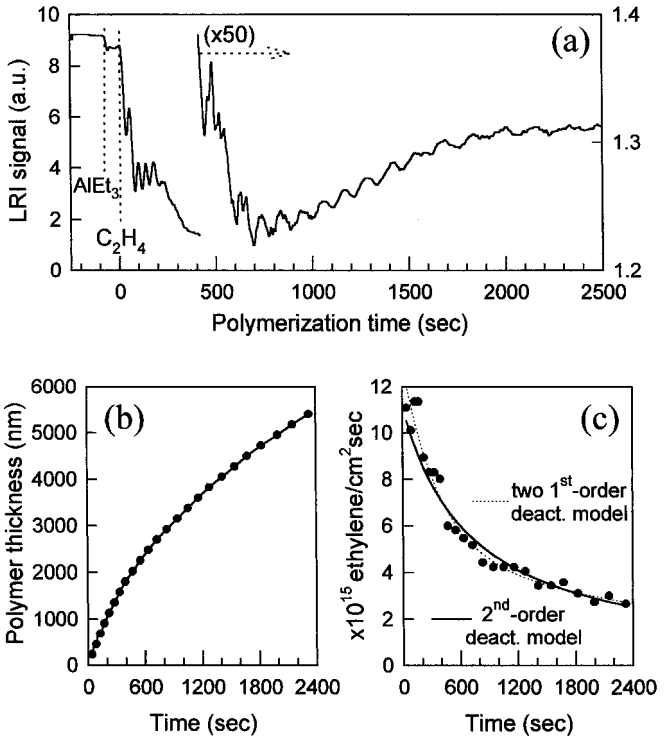

FIG. 2. (a) LRI signal, (b) polymer film thickness $d_m(t_m)$, and (c) polymerization rate as a function of time during the ethylene polymerization on a $TiCl_x/MgCl_2$ model catalyst. Polymerization was performed with 900 Torr of ethylene in the presence of the $AlEt_3$ (5 Torr) in the gas phase. The reactor temperature was kept at 340 K. In (c), the density of the polyethylene film produced was assumed to be 0.96. The dotted and solid lines were fitted results with a two-site first-order deactivation model and a second-order deactivation model, respectively. (See text.)

As the polymerization occurred on the $TiCl_x/MgCl_2$ film, the LRI signal intensity changed in an oscillating manner. Figure 2a shows the LRI signal changes as a function of time in ethylene polymerization on the $TiCl_x/MgCl_2$ catalyst film. The polymerization was carried out with 5 Torr $AlEt_3$ (co-catalyst) and 900 Torr ethylene at 340 K. The periodicity of each interference fringe in LRI increased gradually over time. The peak intensities of the interference oscillations that follow one another decreased in a complex way due to light scattering on or in the PE film. It appeared that the ethylene polymerization rate was faster than the polymer chain flow rate, responsible for crystallization or close packing of the PE particles, so that the whole polymer morphology developed some surface roughness or porosity (14).

The growth rate of the PE film thickness was decreased over time as shown in Fig. 2b. The amount of polymer produced on the model catalyst could be calculated using Eq. [2]. Assuming a constant density of the PE film ($d = 0.96$) during the growth, the nominal turnover rate of the polymerization was calculated and is plotted in Fig. 2c. After 40 min of polymerization, the nominal turnover frequency was decreased by ~70%.

The model catalyst was also active for propylene polymerization. Figure 3a depicts the LRI signal changes as a function of time in propylene polymerization on the $TiCl_x/MgCl_2$ catalyst film. The polymerization was carried out with 5 Torr $AlEt_3$ (co-catalyst) and 900 Torr propylene at 340 K. As in the case of ethylene polymerization, the polymerization rate decreased slowly as the polypropylene grew. However, in contrast to the ethylene polymerization, the peak intensities of the interference fringes during the propylene polymerization were almost the same as the initial intensity, indicating that the PP film had a smooth surface and did not cause significant laser scattering.

The $TiCl_x/MgCl_2$ model catalyst could grow a polymer film composed of thin layers of different polymers. Figure 3b shows the LRI signal changes as a function of time during the sequential polymerization of (i) ~230-nm-thick PP film and (ii) ~770-nm-thick PE film on the catalyst film preactivated with $AlEt_3$. The monomer pressures were 900 Torr in both cases and no $AlEt_3$ was present in the gas phase.

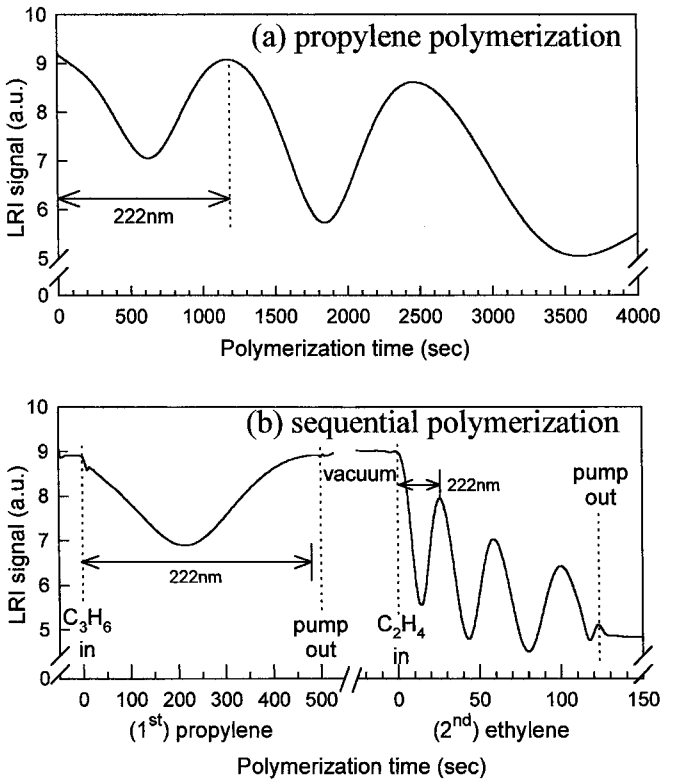

FIG. 3. (a) LRI signal as a function of time during the propylene polymerization on a $TiCl_x/MgCl_2$ model catalyst. Polymerization was performed with 900 Torr of propylene in the presence of the $AlEt_3$ (5 Torr) in the gas phase. (b) LRI signal as a function of time during the sequential polymerization—propylene polymerization followed by ethylene polymerization—on a $TiCl_x/MgCl_2$ model catalyst (note the change in the time scale). The model catalyst was activated by exposure to 5 Torr of $AlEt_3$. Polymerization was performed without the $AlEt_3$ co-catalyst in the gas phase. The monomer pressure was 900 Torr for both propylene and ethylene. The polymerization temperature was 340 K.

When propylene was pumped out, the polymerization process stopped immediately. Upon introduction of ethylene, the polymerization resumed immediately. The shorter periodicity in the LRI signal oscillation resulted from the faster polymerization rate of ethylene (see the next section) compared to propylene.

B. Initial Polymerization Rates and Deactivation

The initial polymerization rates of propylene and ethylene measured in Fig. 3b were compared here. Because the same catalyst was used, there was no uncertainty about the active site concentration in this comparison. The growth of ~230-nm-thick PP film took ~500 s, which corresponded to an average growth rate of 0.46 nm/s. Assuming the PP film density to be 0.91, this growth rate corresponded to a polymerization rate of 4.1×10^{-8} g C_3H_6/cm^2 catalyst · s. In the case of PE, the first 222 nm grew in 25 s, yielding 8.9 nm/s. With a typical PE density of 0.96, this rate corresponded to 8.5×10^{-7} g C_2H_4/cm^2 catalyst · s. These polymerization rates corresponded to nominal turnover frequencies of 6×10^{14} C_3H_6 molecules per square centimeter of catalyst per second and 1.8×10^{16} C_2H_4 molecules per square centimeter of catalyst per second, respectively. The propylene polymerization rate was about 30 times slower than the ethylene polymerization rate on the same catalyst.

Converted with a typical surface area of industrial catalysts (~50 m^2/g), the polymerization activities of the model catalysts in Figs. 2 and 3 corresponded to 40–80 g PP/g catalyst · h · atm and 800–1500 g PE/g catalyst · h · atm, respectively. Industrial catalysts produce about 100–500 g PP/g catalyst · h · atm and 2000–10,000 g PE/g catalyst · h · atm (1, 15). While the precise values were difficult to compare due to the differences in catalyst preparation and polymerization conditions, we concluded that the model catalyst displays a polymerization activity on the same order of magnitude as its industrial counterparts.

The polymerization activity of the model catalyst decreased as the polymerization continued. This is a common feature of the supported Ziegler–Natta polymerization catalysts (1, 2). The decay of the polymerization rate could be fitted with simple kinetic models (2). In Fig. 2c, the dotted line was fitted with a combination of two first-order deactivation curves and the solid line was fitted to a second-order deactivation model. Both models fit the data well. These fitting results have been interpreted in the literature as first-order decay processes of two different active sites (16) or bimolecular decay processes such as a coupling reaction of two adjacent sites (2). However, these models considered only chemical aspects of the alteration of active sites and not the physical aspects of the monomer transport through the polymer layer. The polymerization occurred at the bottom of the polymer layer and the monomer molecules in the gas phase must diffuse through the polymer layer to the active sites (17). As the polymer film grew thicker, the diffusion barrier for monomer transport to the active sites would be expected to increase, lowering the polymerization rate (18, 19). The diffusion limitation could be a dominant factor after a significant degree of polymerization.

It also should be noted that the morphology of the polymer film changed in a complex way as a function of polymerization time. In Fig. 2a, the peak intensity of the LRI oscillation decreased significantly for the first 25 s, remained constant until $t = \sim 200$ s, and then decreased again for the next ~400 s. This decrease in the oscillation peak intensity was caused by roughness of the polymer film surface, inhomogeneity in the film density, or porosity of the film. From $t = \sim 700$ s, the peak intensities of the oscillation increased slightly over a long period of time. This could indicate that the pores in the film were filled or that the film surface became smoother as the polymerization continued (18). These complicated changes in the polymer morphology must be considered in kinetic modeling and theoretical simulations of monomer transport in order to understand the nature of deactivation in the heterogeneous Ziegler–Natta polymerization system. More experiments exploring changes in surface morphology using atomic force microscopy as a function of polymerization time would be useful.

IV. CONCLUSIONS

The Ziegler–Natta polymerization of ethylene and propylene on a small-surface-area model catalyst has been monitored with laser reflection interferometry. The LRI technique measured the thickness of the polymer film growing on the model catalyst during the polymerization. With reasonable assumptions for the polymer film density, the film growth rate could be converted to the polymerization rate. In addition, information about the changes in the polymer film morphology during the polymerization could be obtained indirectly from the peak intensity changes in LRI as a function of time. The $TiCl_x/MgCl_2$ model catalysts have been proven to have activities that are on the same order of magnitude as those of the industrial, high-surface-area catalysts.

ACKNOWLEDGMENTS

This work was supported by the Director, Office of Energy Research, Office of Basic Energy Sciences, Material Science Division, of the U.S. Department of Energy under Contract DE-AC03-76SF00098. The authors also acknowledge support from Montell USA, Inc.

REFERENCES

1. Barbe, P. C., Cesshin, G., and Noristi, L., *Adv. Polym. Sci.* **81**, 1 (1986).
2. Dusseault, J. J. A., and Hsu, C. C., *J.M.S.-Rev. Macromol. Chem. Phys.* **C33**, 103 (1993).
3. Thune, P. C., Loos, J., Lemstra, P. J., and Niemantsverdriet, J. W., *J. Catal.* **183**, 1 (1999).
4. Korani, T., Magni, E., and Somorjai, G. A., *Top. Catal.* **7**, 179 (1999).
5. Kim, S. H., and Somorjai, G. A., *J. Phys. Chem.* **100** (2000).

6. Magni, E., and Somorjai, G. A., *Surf. Sci.* **341**, L1078 (1995).
7. Kim, S. H., and Somorjai, G. A., *Appl. Surf. Sci.*, in press.
8. Kim, S. H., Tewell, C. R., and Somorjai, G. A., submitted for publication.
9. Zuiker, C. D., Gruen, D. M., and Krauss, A. R., *MRS Bull.* **20**(5), 29 (1995).
10. Galiatsatos, V., Neaffer, R. O., Sen, S., and Sherman, B. J., *in* "Physical Properties of Polymer Handbook" (J. E. Mark, Ed) p. 535. Am. Inst. of Phys., New York, 1996.
11. Fuchs, O., Bohn, L., Fleissner, M., Gann, G., Suhr, H. H., and Schuddemage, H. D. R., *in* "Ethylene and Propylene Polymers" (F. D. Snell and L. S. Ettf, Eds.), Vol. 12, p. 350. Wiley, New York, 1971.
12. Brandrup, J., and Immergut, E. H., "Polymer Handbook." Wiley, New York, 1975.
13. Stehling, F. C., and Mandelkern, L., *Macromolecules* **3**, 242 (1970).
14. In atomic force microscopic measurements of the sequential polymerized PP/PE film of a total thickness of ~900 nm, the rms roughness was about 100 nm for a 10 μm $\times$ 10 μm area.
15. Keii, T., and Soga, K., "Catalytic Olefin Polymerization." Elsevier, Amsterdam, 1990.
16. Tait, P. J. T., and Wang, S., *Polym. J.* **20**, 499 (1998).
17. Kim, S. H., and Somorjai, G. A., submitted for publication.
18. Hamba, M., Han-Adebekun, G. C., and Ray, W. H., *J. Polym. Sci. Pol. Chem.* **35**, 2075 (1997).
19. Lim, S.-Y., and Choung, S.-J., *Appl. Catal. A* **153**, 103 (1997).